DALTON
FULL PAPER

Ternary adduct $\{[W(CN)_8]^{3-},[Pt(en)_2]^{2+},[W(CN)_8]^{3-}\}$ in aqueous solution and crystal structure of $[Pt(en)_2]_3[W(CN)_8]_2{\cdot}4H_2O$ with infinite linear W · · · Pt chains

Robert Podgajny, Barbara Sieklucka * and Wiesław Łasocha

Faculty of Chemistry, Jagiellonian University, Ingardena 3, 30-060 Kraków, Poland. E-mail: siekluck@chemia.uj.edu.pl

Received 24th January 2000, Accepted 17th April 2000

A new donor–acceptor system based on $[W(CN)_8]^{3-}$ and $[Pt(en)_2]^{2+}$ has been characterised in aqueous solution and in the solid state. Spectroscopic studies indicate formation of the ternary adduct $\{[W(CN)_8]^{3-},[Pt(en)_2]^{2+},[W(CN)_8]^{3-}\}$ in aqueous solution. The aggregate has been described as a mixed-valence species with weak-to-moderate coupling between metal centres. The solid $[Pt(en)_2]_3[W(CN)_8]_2{\cdot}4H_2O$ exhibits the simultaneous presence of $\{W^V, Pt^{II}, W^V\} \longleftrightarrow \{W^{IV}, Pt^{IV}, W^{IV}\}$ electronic isomers and can be interpreted in terms of ground state borderline electronic localised-to-delocalised species. The structure of $[Pt(en)_2]_3[W(CN)_8]_2{\cdot}4H_2O$ consists of one-dimensional infinite chains formed by tungsten and platinum moieties linked through hydrogen bonding from ethane-1,2-diamine nitrogens and water molecules to nitrogens of all cyano ligands.

Introduction

The recent investigations of the chemistry of bridged mixed-valence compounds frequently give evidence for borderline systems between the limiting localised and delocalised descriptions.[1] In mixed-valence binuclear complexes $[(NC)_5FeLRu(NH_3)_5]^n$ the presence of $[Ru^{II}–L–Fe^{III}]$ and $[Ru^{III}–L–Fe^{II}]$ electronic isomers has been established.[2] The crucial role of the more reactive electronic isomers $[Ru^{II}–L–Fe^{III}]$ present in binuclear $[Ru^{II}–L–Fe^{III}]$ bridged systems in their redox reactivity has been investigated thoroughly.[3] The first spectroscopic and X-ray evidence for the non-bridged heterobinuclear mixed-valence $[Pt(NH_3)_4]_2[W(CN)_8][NO_3]{\cdot}2H_2O$ complex that exists as a borderline localised-to-delocalised system has been found in our previous studies.[4,5] The substantial electronic delocalisation has been created by the stereochemical barrier to the inner-sphere two-electron oxidation of $[Pt(NH_3)_4]^{2+}$ by $[W(CN)_8]^{3-}$. We have extended this work to the $[Pt(en)_2]^{2+}–[W(CN)_8]^{3-}$ system. We present here a spectroscopic analysis of the mixed-valence species in solution and in the solid state together with the crystal structure of $[Pt(en)_2]_3[W(CN)_8]_2{\cdot}4H_2O$. In aqueous solution the system is characterised as hydrogen bonded $\{[W(CN)_8]^{3-},[Pt(en)_2]^{2+},[W(CN)_8]^{3-}\}$ ternary aggregates. In the crystal $[Pt(NH_3)_4]^{2+}$ and $[W(CN)_8]^{3-}$ ions are linked by hydrogen bonds giving rise to linear infinite Pt · · · W chains. From spectroscopic characteristics $[Pt(en)_2]_3[W(CN)_8]_2{\cdot}4H_2O$ was found to exhibit ground state borderline electronic localised-to-delocalised properties.

Experimental

Materials

The compound $K_3[W(CN)_8]{\cdot}1.5H_2O$ was prepared according to the published procedure;[6] $[Pt(en)_2]Cl_2$ was obtained from Aldrich and used without further purification. All other materials were of analytical grade (Aldrich) used as supplied.

Synthesis of tris[bis(ethane-1,2-amine)platinum(II)] bis[octacyanotungstate(V)] tetrahydrate, $[Pt(en)_2]_3[W(CN)_8]_2{\cdot}4H_2O$

Combination of equimolar aqueous solutions of colourless $[Pt(en)_2]Cl_2$ (77.2 mg, 0.2 mmol, 1 cm^3) and of yellow $K_3[W(CN)_8]$ (107.2 mg, 0.2 mmol, 1 cm^3) (Pt : W = 1 : 1 v/v) resulted in the immediate appearance of a violet colour. Crystals suitable for X-ray measurements were grown for a few weeks from the solution, protected from incident light at room temperature. They were collected by suction filtration, washed three times with water and dried in air. The isolated red crystals were identified as $[Pt(en)_2]_3[W(CN)_8]_2{\cdot}4H_2O$. Yield: 11 mg, 6% (Found: C, 19.33; H, 3.08; N, 21.80. Calc. for $C_{28}H_{56}N_{28}O_4Pt_3W_2$: C, 18.66; H, 3.11; N, 21.75%). The solid is practically insoluble in water and in common organic solvents.

Instrumentation and techniques

The UV/VIS spectra were recorded on a Shimadzu 2101 PC spectrophotometer, diffuse reflectance spectra of solid samples as dispersions in $BaSO_4$ on a Shimadzu 2101 PC equipped with a Shimadzu ISR-260 integrating-sphere assembly using a $BaSO_4$ disc as reference. The IR spectra on a Bruker model FT-IFS 47 spectrometer in KBr pellets, FT-Raman on a Bio-Rad Raman Accessory model 60N coupled with a Bio-Rad step-scan interferometer model FTS 6000 furnished with a cold (liquid nitrogen) germanium detector equipped with a Nd:YAG cw laser (Spectra-Physics). The ESR spectra were recorded on Varian and Bruker ELEXSYS EPR spectrometers at 9.5 GHz microwave frequency (298 and 77 K) in the range 3000–4000 G. The cyclic voltammetry measurements were performed with multipurpose electrochemical analyser EA9 (MTM). A standard three-electrode configuration with a platinum working and counter electrode and a Ag–AgCl reference electrode was used. The stoichiometry of the adduct formed, the overall equilibrium constant and molar absorption coefficient were determined spectrophotometrically. The mole ratio $[Pt(en)_2]^{2+}$: $[W(CN)_8]^{3-}$ has been established by the Job method, varying the molar ratio of the two species in solution while keeping the total moles constant. The overall equilibrium constant and molar absorption coefficient of the adduct were determined from the absorbance data A_{535} *vs.* the equimolar concentration of reactants, c_{tot}. The experiments were done at 535 nm, $I = 0.45$ mol dm^{-3} (KCl), 25 °C. Assuming the experimentally determined equilibrium (eqn. 1) for the form-

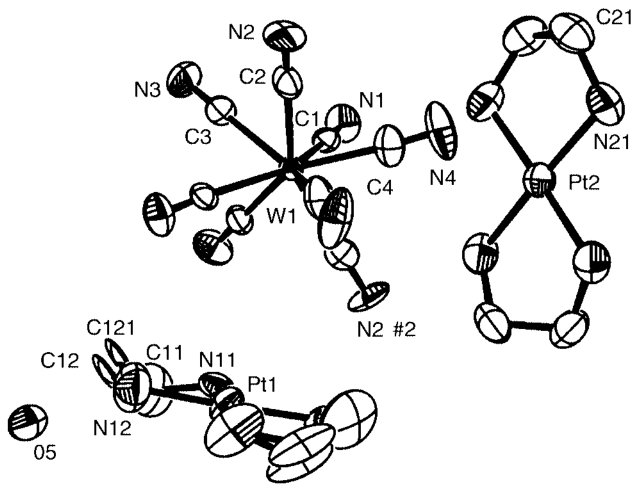

Fig. 1 An ORTEP[9] drawing of the independent unit of the crystal structure of $[Pt(en)_2]_3[W(CN)_8]_2{\cdot}4H_2O$ showing the atom numbering scheme. All atoms are represented by 50% probability ellipsoids.

ation of the ternary aggregate (see below), the measured total absorbance of the equimolar mixture of reagents is represented by $A_{535} = \varepsilon_{Pt}(c_{tot} - c_{tri}) + \varepsilon_W(c_{tot} - 2c_{tri}) + \varepsilon_{tri}c_{tri}$, where c_{tot} and c_{tri} are the concentration of $[W(CN)_8]^{3-}$ and $[Pt(en)_2]^{2+}$ ions and of $\{[W(CN)_8]^{3-},[Pt(en)_2]^{2+},[W(CN)_8]^{3-}\}$, respectively, and ε_{Pt}, ε_W and ε_{tri} are the molar absorption coefficients of $[Pt(en)_2]^{2+}$, $[W(CN)_8]^{3-}$ and triplet species, respectively. The overall equilibrium constant K_{OS} is expressed by $c_{tri}/[(c_{tot} - c_{tri})(c_{tot} - 2c_{tri})^2]$. The combination of the above equations (assuming $c_{tri}^3 \approx 0$) gives the expression $A_{535} = c_{tot}(\varepsilon_{Pt} + \varepsilon_W) + \{(\varepsilon_t - \varepsilon_{Pt} - 2\varepsilon_W)[1 + 5K_{OS}c_{tot}^2 - (-7K_{OS}^2c_{tot}^4 + 10K_{OS}c_{tot}^2 + 1)^{1/2}]\}/16K_{OS}c_{tot}$. The K_{OS} and ε_{tri} values were determined using a non-linear least-squares fitting procedure.

Spectral deconvolution of electronic spectra in the visible region was performed by using the Gaussian Fit Multi-peaks function within Microsoft Origin 5.0, which decomposes absorbance *vs.* wavenumber (cm^{-1}) data into single Gaussian bands.

Crystal structure analysis

Data were collected with a KM-4 diffractometer, with graphite-monochromated Mo-Kα radiation and ω–2θ scans. The structure was solved by the PATT option of the SHELXS 97[7] program; all non-hydrogen atoms were found by successive Fourier syntheses. Details of the crystal structure solution and refinement are presented in Table 1. The positions of hydrogen atoms were calculated with full matrix least-squares refinement on F^2, anisotropic for all but hydrogen and isotropic refinement for hydrogen atoms were performed with SHELXL 97.[8]

CCDC reference number 186/1941.

See http://www.rsc.org/suppdata/dt/b0/b000645i/ for crystallographic files in .cif format.

Table 1 Crystal data and structure refinement for $[Pt(en)_2]_3[W(CN)_8]_2{\cdot}4H_2O$

Empirical formula	$C_{28}H_{56}N_{28}O_4Pt_3W_2$
Formula weight	1802.06
Crystal system	Orthorhombic
Space group	*Fddd* (no. 70)
a/Å	18.329(3)
b/Å	20.302(5)
c/Å	27.084(7)
V/Å^3	10078(4)
Z, D_c/Mg m^{-3}	8, 2.365
T/K	298(2)
μ/mm^{-1}	12.909
Measured/independent reflections [$I > 2\sigma(I)$]	5297/2747 [*R*(int) = 0.0818]
Final *R*1/*wR*2	0.0574/0.1429

Table 2 Selected bond lengths [Å] and angles [°] for $[Pt(en)_2]_3[W(CN)_8]_2{\cdot}4H_2O$

$[W(1)(CN)_8]^{3-}$			
W(1)–C(1)	2.176(13)	C(1)–N(1)	1.112(17)
W(1)–C(2)	2.168(17)	C(2)–N(2)	1.122(19)
W(1)–C(3)	2.137(14)	C(3)–N(3)	1.162(18)
W(1)–C(4)	2.148(15)	C(4)–N(4)	1.135(18)
N(1)–C(1)–W(1)	176.1(14)	N(3)–C(3)–W(1)	179.0(13)
N(2)–C(2)–W(1)	178.3(14)	N(4)–C(4)–W(1)	177(2)
$[Pt(1)(en)_2]^{2+}$			
Pt(1)–N(11)	2.037(12)	N(11)–C(11)	1.50(2)
Pt(1)–N(11)#4	2.037(12)	N(12)–C(12)	1.46(3)
Pt(1)–N(12)	2.024(16)	C(11)–C(12)	1.492(16)
Pt(1)–N(12)#4	2.024(16)	N(12)–C(121)	1.46(3)
		C(11)–C(121)	1.495(16)
C(11)–N(11)–Pt(1)	108.2(13)		
C(12)–C(11)–N(11)	112.1(18)	C(121)–C(11)–N(11)	100.2(19)
N(12)–C(12)–C(11)	112(2)	N(12)–C(121)–C(11)	112(2)
C(12)–N(12)–Pt(1)	113.0(15)	C(121)–N(12)–Pt(1)	104.7(15)
N(12)–Pt(1)–N(11)	84.1(7)		
N(12)–Pt(1)–N(12)#4	94.1(12)		
N(11)#4–Pt(1)–N(11)	97.7(7)		
N(12)–Pt(1)–N(11)#4	177.0(8)		
		C(12)–N(12)–C(121)	16.5(15)
		C(12)–C(11)–C(121)	16.2(14)
$[Pt(2)(en)_2]^{2+}$			
Pt(2)–N(21)	2.009(13)	N(21)–C(21)	1.50(2)
		C(21)–C(21)#2	1.51(3)
C(21)–N(21)–Pt(2)	112.3(9)	N(21)#2–Pt(2)–N(21)#1	175.7(8)
N(21)–C(21)–C(21)#2	107.8(9)		
N(21)–Pt(2)–N(21)#2	82.8(8)	N(21)–Pt(2)–N(21)#1	97.4(8)

Symmetry transformations used to generate equivalent atoms: #1 $-x + \frac{3}{4}, -y + \frac{3}{4}, z$; #2 $-x + \frac{3}{4}, y, -z + \frac{7}{4}$; #3 $x, -y + \frac{3}{4}, -z + \frac{7}{4}$; #4 $x, -y + \frac{1}{4}, -z + \frac{5}{4}$.

Results and discussion

Crystal structure of $[Pt(en)_2]_3[W(CN)_8]_2{\cdot}4H_2O$

The orthorhombic $[Pt(en)_2]_3[W(CN)_8]_2{\cdot}4H_2O$ contains isolated $[Pt^{II}(en)_2]^{2+}$, $[W^V(CN)_8]^{3-}$ ions and H_2O molecules linked through a hydrogen bond network, electrostatic forces and van der Waals interaction. The independent part of the crystal structure and mutual orientation of tungsten and platinum complexes are presented in Fig. 1. Selected bonds and angles are presented in Table 2. The geometry of $[W(CN)_8]^{3-}$ is halfway between those of a dodecahedron D_{2d} and square antiprism D_{4d} (D_2 point group, site symmetry 2). The mean values of W–C [2.157(15) Å], C–N [1.132(18) Å] distances and W–C–N [177.6(14)°] angles are in very good agreement with those of other octacyanotungstate(v) compounds.[5,10] The average Pt–N, C–N and C–C distances in $[Pt(1)(en)_2]^{2+}$ and $[Pt(2)(en)_2]^{2+}$ cations of Λ conformation are comparable with those found for other platinum complexes with ammine and polyammine ligands.[11] Within the Pt(1) complex we found the C(12) atom of an en ligand to be in a state of permanent disorder, occupying two different positions [C(12) and C(121)]. The platinum–tungsten separations are 5.215(1) Å for Pt(1)···W(1) and 6.287(3) Å for Pt(2)···W(1). The characteristic feature of the mutual orientation of Pt(1) and W(1) is the cyano ligand pointing roughly towards the axial direction of Pt(1) [Pt(1)···N(2#2) separation of 3.934(14) Å]. This arrangement can be interpreted in terms of an intermediate structure between purely ionic and cyano bridged species. In the crystal the three-dimensional hydrogen bonding network involves bonding from ethane-1,2-diamine and water molecules to nitrogens of all cyano ligands (Table 3). These connections form infinite one-dimensional tungsten–platinum chains, aligned along the [010] and [110] directions (Fig. 2).

Table 3 The distances [Å] and angles [°] of possible hydrogen bonds for $[Pt(en)_2]_3[W(CN)_8]_2\cdot 4H_2O$

Donor–H	Donor···Acceptor	H···Acceptor	Donor–H···Acceptor
N21–H21A	N21···N4 (1)	H21A···N4 (1)	N21–H21A···N4 (1)
0.900(0.013)	2.958(0.018)	2.060(0.013)	175.32(0.86)
1.030[a]		1.931[a]	175.01[a]
N21–H21B	N21···N2 (2)	H21B···N2 (2)	N21–H21B···N2 (2)
0.900(0.013)	3.016(0.019)	2.225(0.013)	146.44(0.92)
1.030		2.118	144.49
N11–H11B	N11···N2 (3)	H11B···N2 (4)	N11–H11B···N2 (4)
0.900(0.013)	2.956(0.020)	2.148(0.014)	149.09(0.92)
1.030		2.037	147.22
N12–H12A	N12···O5 (4)	H12A···O5 (5)	N12–H12A···O5 (5)
0.900(0.022)	2.912(0.030)	2.018(0.020)	172.30(1.49)
1.030		1.889	171.77
N12–H12B	N12···O5 (5)	H12B···O5 (6)	N12–H12B···O5 (6)
0.900(0.023)	2.984(0.030)	2.227(0.021)	141.46(1.41)
1.030		2.126	139.27
O5–H51	O5···N3 (6)	H51···N3 (8)	O5–H51···N3 (8)
0.952(0.157)	2.876(0.019)	2.240(0.143)	123.35(9.79)
0.938		2.248	123.65
O5–H52	O5···N1 (7)	H52···N1 (10)	O5–H52···N1 (10)
0.954(0.147)	3.030(0.025)	2.448(0.218)	119.22(11.29)
0.938		2.456	119.54

Number of possible hydrogen bonds 7. Equivalent positions: (1) $-x + \frac{3}{4}, +y, -z + \frac{3}{4} + 1$; (2) $x + \frac{1}{4}, -y + 1, +z + \frac{1}{4}$; (3) $-x + \frac{3}{4}, +y - \frac{1}{2}, -z + \frac{1}{4} + 1$; (4) $-x + \frac{3}{4}, +y, -z + \frac{3}{4}$; (5) $x - \frac{1}{2}, -y + \frac{1}{4}, -z + \frac{3}{4}$; (6) $x + \frac{1}{4}, -y + \frac{1}{2}, +z - \frac{1}{4}$; (7) $-x + \frac{1}{4} + 1, +y - \frac{1}{2}, -z + \frac{3}{4}$. [a] Values normalised following ref. 22.

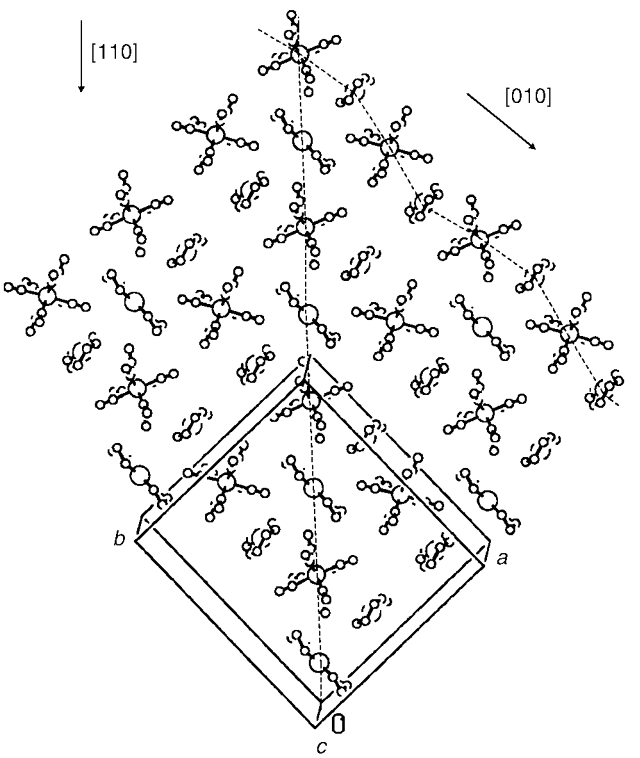

Fig. 2 A PLUTON[12] packing diagram of $[Pt(en)_2]_3[W(CN)_8]_2\cdot 4H_2O$ presenting the linear arrangement of $[W(CN)_8]^{3-}$ and $[Pt(en)_2]^{2+}$ ions in [010] and [110] directions. Broken lines: infinite Pt···W chains. Water molecules are omitted for clarity.

Spectroscopic characterisation of the $[W(CN)_8]^{3-}$ mixed-valence ternary species $\{[W(CN)_8]^{3-},[Pt(en)_2]^{2+},[W(CN)_8]^{3-}\}$ in aqueous solution

On mixing a solution of $[W(CN)_8]^{3-}$ with $[Pt(en)_2]^{2+}$ an intense violet colour appears (Fig. 3). The solution exhibits spectroscopic transitions at λ_{max} 430 and 535 nm. The former can be assigned either to LMCT $b_2(\sigma) \longrightarrow a_1(d_{z^2})$ of $[W(CN)_8]^{4-}$ or to LF $b_1(d_{x^2-y^2}) \longrightarrow a_1(d_{z^2})$ of $W(CN)_8]^{3-}$ transitions.[13] The 535 nm transition is not present in either reduced or oxidised form of either complex alone and considering previous evidence with the $[W(CN)_8]^{3-}$–$[Pt(NH_3)_4]^{2+}$ donor–acceptor system[4] we assign it to an optical MMCT (metal-to-metal charge-transfer) transition from $[Pt(en)_2]^{2+}$ donor to $[W(CN)_8]^{3-}$ acceptor. The stoichiometry of the adduct formed Pt : W = 1 : 2 has been established by the Job plot, shown in the

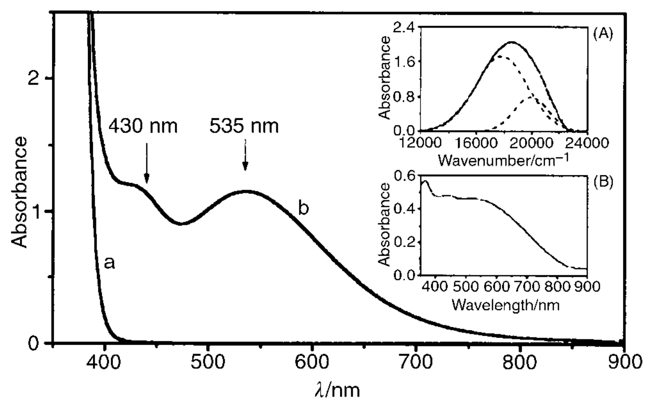

Fig. 3 Electronic spectra of (a) $K_3[W(CN)_8]$ (1.5×10^{-2} mol dm^{-3}), (b) an equimolar mixture of $K_3[W(CN)_8]$ and $[Pt(en)_2]Cl_2$ ($c_{tot} = 1.5 \times 10^{-2}$ mol dm^{-3}). Inset (A): spectral deconvolution of the MMCT band at 535 nm. Inset (B): diffuse reflectance spectrum of solid $[Pt(en)_2]_3$-$[W(CN)_8]_2\cdot 4H_2O$.

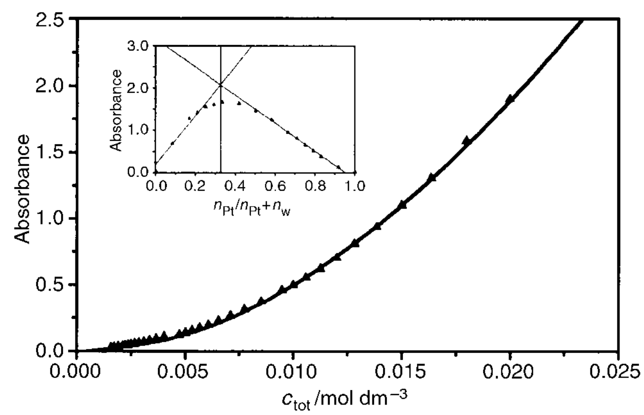

Fig. 4 Dependence of absorbance A_{535} on concentration (c_{tot}) of the equimolar mixture of $[W(CN)_8]^{3-}$ and $[Pt(en)_2]^{2+}$ ions in aqueous solution. Inset: Job plot of $[Pt(en)_2]^{2+}$–$[W(CN)_8]^{3-}$ system ($T = 298$ K, $I = 0.45$ mol dm^{-3}, KCl).

Table 4 IR and Raman spectral data (cm^{-1}) of $[Pt(en)_2]_3[W(CN)_8]_2\cdot 4H_2O$

IR	Raman	Assignment
3594s, 3525s, 3437s		ν(OH)
3315s, 3067vs		$\nu(NH_2)$, ν(CH)
2152vw, 2145vw(sh)	2158vw, 2147vw(sh)	ν(CN) [W^V]
2138w	2137s	ν(CN) [W^V and W^{IV}]
2129s, 2124s, 211vvw, 2100s(sh), 2095vs, 2072vw, 2055w	2127m, 2112m, 2099s, 2075w, 2060w	ν(CN) [W^{IV}]
1618s	1599w	$\nu(NH_2)$, ν(OH)
1601s, 1584m, 1452m, 1401vw, 1369m, 1325m, 1306w, 1293w, 1274w, 1186w, 1157s, 1132m, 1049s, 1022w, 996w	1461vw, 1397vw, 1325vw, 1277vw, 1207vw, 1168vw, 1086vw, 1055vw	{$\delta(CH_2)$, $\delta(NH_2)$, $\gamma(CH_2)$, $\omega(CH_2)$, $\gamma(NH_2)$, $\omega(CH_2)$, ν(CC), ν(NC)}
898w, 881w, 820w, 803w	885w, 830vw	$\nu(CH_2)$, $\rho_r(NH_2)$
583w, 556vw, 542m, 485w	586mw, 573mw, 544w, 531vw(sh), 517vw(sh), 484mw	ν(PtN)[a], ν(NPtN)[b]
471w		ν(WC), [W^{IV}]
450w, 432w	451vw	ν(WC) [W^V]
	405vw	ν(WC) [W^V and W^{IV}]
	351vw, 320vw, 278mw, 268mw, 206vw	δ(NPtN)[a]

[a] Ref. 4. [b] Ref. 20.

inset of Fig. 4. The solution equilibrium contains the hydrogen-bonded (see above) ternary adduct $\{[W(CN)_8]^{3-},[Pt(en)_2]^{2+},[W(CN)_8]^{3-}\}$, which forms according to eqn. (1). The formation

$$[Pt^{II}(en)_2]^{2+} + 2[W^V(CN)_8]^{3-} \xrightleftharpoons{K_{OS}} \{[W^V(CN)_8]^{3-},[Pt^{II}(en)_2]^{2+},[W^V(CN)_8]^{3-}\} \quad (1)$$

of hydrogen-bonded multiple ion clusters of $[M(CN)_6]^{n-}$ cyano complexes [M = Fe^{II}, Co^{III}, Ru^{II} or Os^{II}] with ruthenium(III) ammine cations[14] and ternary aggregates of ruthenium cyano and ethylenediamine complexes[15] have been demonstrated recently.

The spectroscopic MMCT transition of $\{[W(CN)_8]^{3-},[Pt(en)_2]^{2+},[W(CN)_8]^{3-}\}$ ion triplet corresponds to the electron-transfer process shown in eqn. (2). The Beer's law plot

$$\{[W^V(CN)_8]^{3-},[Pt^{II}(en)_2]^{2+},[W^V(CN)_8]^{3-}\} \xrightarrow{h\nu} \{[W^{IV}(CN)_8]^{4-},[Pt^{III}(en)_2]^{3+},[W^V(CN)_8]^{3-}\} \quad (2)$$

for MMCT at 535 nm of the $\{[W^V(CN)_8]^{3-},[Pt^{II}(en)_2]^{2+},[W^V(CN)_8]^{3-}\}$ adduct is shown in Fig. 4. From the strongly curved plot the overall formation constant K_{OS} and molar absorption coefficient ε_{tri} were determined as $(1.4 \pm 0.1) \times 10^3$ $dm^6\ mol^{-2}$ and $458 \pm 19\ dm^3\ mol^{-1}\ cm^{-1}$, respectively ($T = 298$ K, $I = 0.45\ mol\ dm^{-3}$ (KCl)). Spectral deconvolution analysis of the MMCT band shows two peaks at λ_{max} 560 and 500 nm (17 857 and 19 988 cm^{-1}, respectively) [inset (A) in Fig. 3]. We attribute these two MMCT transitions to the two different W···Pt separations of 5.215 and 6.287 Å, respectively (see above) although the formation of higher order adducts, which could be responsible for the appearance of higher energy bands, cannot be excluded.[14,15]

The application of the Hush model[16] to the above spectroscopic interpretation of the MMCT band coupled with the determined W···Pt separations allows one to estimate the electronic coupling matrix element H_{ab} between the platinum(II) and tungsten(V) centres. The values of 693 and 494 cm^{-1} for 5.215 (ν_{max} 17 845 cm^{-1}, $\nu_{1/2} = 3\ 781\ cm^{-1}$) and 6.287 Å ($\nu_{max}$ 19 988 cm^{-1}, $\nu_{1/2} = 2493\ cm^{-1}$) respectively, indicate a valence-trapped adduct, with weak-to-moderate coupling between metal centres. The H_{ab} values are consistent with those obtained for $[Pt(NH_3)_4]^{2+}$–$[W(CN)_8]^{3-}$ system,[4] ternary aggregates of ruthenium cyano and ethylenediamine complexes[11] and cyanide-bridged complexes.[17]

Cyclic voltammetric results show one isolated quasi-reversible wave at +0.32 mV *vs.* Ag–AgCl (+0.52 mV *vs.* NHE), close to the value for an isolated $[W(CN)_8]^{3-/4-}$ couple,[18] with 80 mV peak-to-peak separation (0.1 V s^{-1}). The ESR solution spectra of the adduct (at ambient and liquid N_2 temperatures) exhibit a single symmetric signal at $g_{iso} = 1.97$, characteristic of an isolated tungsten(V) centre.[4,19] There is no observable signal from Pt^{III}.

Spectroscopic characterisation of solid $[Pt(en)_2]_3[W(CN)_8]_2\cdot 4H_2O$

The diffuse reflectance spectrum of crystalline $[Pt(en)_2]_3$-$[W(CN)_8]_2\cdot 4H_2O$ [inset (B) in Fig. 3] shows a MMCT band at 522 along with 438 and 365 nm bands, characteristic of $[W(CN)_8]^{4-}$ ion.[13] The correspondence of the electronic bands of solid $[Pt(en)_2]_3[W(CN)_8]_2\cdot 4H_2O$ and the aqueous $\{[W(CN)_8]^{3-},[Pt(en)_2]^{2+},[W(CN)_8]^{3-}\}$ adduct confirms the same type of interaction between metal centres. Table 4 shows the IR and Raman data of $[Pt(en)_2]_3[W(CN)_8]_2\cdot 4H_2O$. The pattern and the range of ν(CN) stretching frequencies are diagnostic of $[W(CN)_8]^{3-}$ and $[W(CN)_8]^{4-}$ superimposed.[4,5] While the ν(CN) values of 2152, 2145, 2138 (IR) and 2158, 2147, 2137 cm^{-1} (Raman) are characteristic of $[W(CN)_8]^{3-}$,[5] 2138 (IR), 2137 (Raman) cm^{-1} and lower frequency ν(CN) bands can be attributed to $[W(CN)_8]^{4-}$. The bands corresponding to the ν(PtN), ν(NPtN) and δ(NPtN) vibrations in the Raman spectrum suggest the presence of platinum-(II) and -(IV) centres.[20] The vibrational characteristics of $[Pt(en)_2]_3$-$[W(CN)_8]_2\cdot 4H_2O$ are diagnostic of the electronic environment of W^V and W^{IV} along with that of Pt^{II} and Pt^{IV}. Analogous strong ground state $Pt^{II} \leftrightarrow W^V$ charge transfer interactions were recently found in $[Pt^{II}(NH_3)_4]_2[W^V(CN)_8][NO_3]\cdot 2H_2O$.[5] The ESR spectra of solid $[Pt(en)_2]_3[W(CN)_8]_2\cdot 4H_2O$ (at ambient and liquid N_2 temperatures) exhibit a single symmetric signal at $g_{iso} = 1.97$, which confirms the presence of W^V in the structure.

The vibrational characteristics together with ESR results pointing out the simultaneous presence of W^{IV} and W^V along with Pt^{II} and Pt^{IV} indicate two electron exchange occurring between Pt^{II} and W^V, $\{W^V, Pt^{II}, W^V\} \leftrightarrow \{W^{IV}, Pt^{III}, W^V\} \leftrightarrow \{W^{IV}, Pt^{IV}, W^{IV}\}$.

Conclusion

The reaction of $[W(CN)_8]^{3-}$ and $[Pt(en)_2]^{2+}$ in aqueous solution led to a $\{[W^V(CN)_8]^{3-},[Pt^{II}(en)_2]^{2+},[W^V(CN)_8]^{3-}\}$ mixed-valence ternary adduct held together by hydrogen bonds. The isolated bimetallic assembly $[Pt(en)_2]_3[W(CN)_8]_2\cdot 4H_2O$ has one-dimensional tungsten–platinum chains formed through hydrogen bonding from ethane-1,2-diamine and water molecules to nitrogens of all cyano ligands. The cyano ligands seems to be blocked by hydrogen bonds on their way towards axial sites of

Pt(1) centres, giving rise to an intermediate arrangement between purely ionic and trimeric cyano bridged species[21] within the chain. The strong electronic coupling provided by the short Pt(1)···W(1) separation of 5.215 Å and hydrogen bond network results in a ground state borderline electronic localised-to-delocalised species.

Acknowledgements

We thank the Polish Research Grants Committee (Grant No. 461/T09/97/13 to B. S.) for support of this research.

References

1 Ch. G. Atwood and W. E. Geiger, *J. Am. Chem. Soc.*, 1993, **11**, 5310; W. Bruns, W. Kaim, E. Waldh and M. Krejcik, *Inorg. Chem.*, 1995, **34**, 663; G. A. Neyhart, C. J. Timpson, W. D. Bates and T. J. Meyer, *J. Am. Chem. Soc.*, 1996, **118**, 3730; T. Ito, T. Hamaguchi, H. Nagino, T. Yamaguchi, J. Washington and C. P. Kubiak, *Science*, 1997, **277**, 660; K. D. Demadis, G. A. Neyhart, E. M. Kober and T. J. Meyer, *J. Am. Chem. Soc.*, 1998, **120**, 7121.

2 A. E. Almaraz, L. A. Gentil, L. M. Baraldo and J. A. Olabe, *Inorg. Chem.*, 1996, **35**, 7718.

3 A. R. Parise, L. M. Baraldo and J. A. Olabe, *Inorg. Chem.*, 1996, **35**, 5080; F. Fagale, N. E. Katz, V. G. Povse and J. A. Olabe, *Polyhedron*, 1998, **18**, 25; P. Forlano, A. R. Parise, M. Videla and J. A. Olabe, *Inorg. Chem.*, 1997, **36**, 564; M. Ketterle, W. Kaim, J. A. Olabe, A. R. Parise and J. Fiedler, *Inorg. Chim. Acta*, 1999, **291**, 66.

4 B. Sieklucka, *J. Chem. Soc.*, *Dalton Trans.*, 1997, 869 and refs. therein.

5 B. Sieklucka, W. Łasocha, L. M. Proniewicz, R. Podgajny and H. Schenk, *J. Mol. Struct.*, 2000, **520**, 155.

6 A. Samotus, *Rocz. Chem.*, 1973, **47**, 265.

7 G. M. Sheldrick, SHELXS 97, Crystal Structure Solution, MSDOS 32-bit version 1986–97, Release 97-1, University of Göttingen, 1997.

8 G. M. Sheldrick, SHELXL 97, Crystal Structure Refinement, MSDOS 32-bit version 1993-7, Release 97-1, University of Göttingen, 1997.

9 C. K. Johnson, ORTEP, Report ORNL-3794, Oak Ridge National Laboratory, Oak Ridge, TN, 1965.

10 L. D. C. Bok, J. G. Leipoldt and S. S. Besson, *Acta Crystallogr.*, *Sect. B*, 1970, **26**, 684.

11 B. Lippert, C. J. L. Lock, B. Rosenberg and M. Zvangulis, *Inorg. Chem.*, 1977, **16**, 1525; B. Lippert, C. J. L. Lock, B. Rosenberg and M. Zvangulis, *Inorg. Chem.*, 1978, **17**, 2971; P. E. Fanwick and J. L. Huckaby, *Inorg. Chem.*, 1982, **21**, 3067; R. Kuroda, S. Neidle, I. M. Ismail and P. J. Sadler, *Inorg. Chem.*, 1983, **22**, 3620; R. J. H. Clark, M. Kurmoo, A. M. R. Galas and M. B. Hursthouse, *J. Chem. Soc.*, *Dalton Trans.*, 1983, 1583; F. P. Fanizzi, G. Natile and M. Lanfrancchi, *J. Chem. Soc.*, *Dalton Trans.*, 1986, 273; M. Zhou, B. W. Pfennig, J. Staiger, D. van Engen and A. B. Bocarsly, *Inorg. Chem.*, 1990, **29**, 2456.

12 A. L. Spek, PLUTON 92, Bijvoet Center for Biomolecular Research, University of Utrecht, 1992.

13 A. Gołębiewski and H. Kowalski, *Theor. Chim. Acta*, 1968, **12**, 293; A. A. Gołębiewski and R. Nalewajski, *Z. Naturforsch.*, *Teil A*, 1972, **27**, 1672; K. R. Butter, T. J. Kemp, B. Sieklucka and A. Samotus, *J. Chem. Soc.*, *Dalton Trans.*, 1986, 1217.

14 V. G. Poulopoulou and H. Taube, *Inorg. Chem.*, 1997, **36**, 2240; V. G. Poulopoulou and H. Taube, *Inorg. Chem.*, 1997, **36**, 4782.

15 J. Yang, D. Seneviratne, G. Arbatin, A. M. Andersson and J. C. Curtis, *J. Am. Chem. Soc.*, 1997, **119**, 5329.

16 N. S. Hush, *Prog. Inorg. Chem.*, 1967, **8**, 391.

17 A. Vogler, A. H. Osman and H. Kunkely, *Coord. Chem. Rev.*, 1985, **64**, 159; M. W. Laidlow and R. G. Denning, *Inorg. Chim. Acta*, 1994, **219**, 121; M. W. Laidlow and R. G. Denning, *Polyhedron*, 1994, **13**, 1875; M. W. Laidlow and R. G. Denning, *Polyhedron*, 1994, **13**, 2337, M. W. Laidlow and R. G. Denning, *J. Chem. Soc.*, *Dalton Trans.*, 1994, 1987; B. W. Pfennig, J. L. Cohen, I. Sosnowski, N. M. Novotny and D. M. Ho, *Inorg. Chem.*, 1999, **38**, 606.

18 B. Nowicka and A. Samotus, *J. Chem. Soc.*, *Dalton Trans.*, 1998, 1021.

19 T. J. Kemp and M. A. Shand, *J. Chem. Soc.*, *Dalton Trans.*, 1988, 285, B. R. McGarvey, *Inorg. Chem.*, 1966, **5**, 476.

20 R. J. H. Clark and P. C. Turtle, *Inorg. Chem.*, 1978, **17**, 2526; R. J. H. Clark and M. Kurmoo, *Inorg. Chem.*, 1980, **19**, 3522, R. J. H. Clark and M. Kurmoo, *J. Chem. Soc.*, *Dalton Trans.*, 1981, 524.

21 R. Podgajny, Y. Dromzée, K. Kruczała and B. Sieklucka, unpublished work.

22 G. A. Jeffrey and L. Lewis, *Carbohydr. Res.*, 1978, **60**, 179; R. Taylor and O. Kennard, *Acta Crystallogr.*, *Sect. B*, 1983, **39**, 133.